IJC Heart & Vasculature 35 (2021) 100842

Contents lists available at ScienceDirect

IJC Heart & Vasculature

journal homepage: www.journals.elsevier.com/ijc-heart-and-vasculature

Increased fibroblast accumulation in the equine heart following persistent atrial fibrillation

Arnela Saljic [a], Merle Friederike Fenner [b,c], Joris Winters [d], Mette Flethøj [b], Caroline Eggert Eggertsen [a], Helena Carstensen [b], Sarah Dalgas Nissen [a], Eva Melis Hesselkilde [a], Arne van Hunnik [d], Ulrich Schotten [d], Ulrik Sørensen [e], Thomas Jespersen [a], Sander Verheule [d], Rikke Buhl [b,*]

[a] Laboratory of Cardiac Physiology, Department of Biomedical Sciences, Faculty of Health and Medical Sciences, University of Copenhagen, Blegdamsvej 3B, DK-2200 Copenhagen, Denmark
[b] Department of Veterinary Clinical Sciences, Faculty of Health and Medical Sciences, University of Copenhagen, Agrovej 8, DK-2630 Taastrup, Denmark
[c] Department of Veterinary and Animal Sciences, Faculty of Health and Medical Sciences, University of Copenhagen, Grønnegårdsvej 7, 1870 Frederiksberg, Denmark
[d] Department of Physiology, Maastricht University, Maastricht, Netherlands
[e] Acesion Pharma ApS, Copenhagen, Denmark

ARTICLE INFO

Article history:
Received 6 January 2021
Received in revised form 30 June 2021
Accepted 6 July 2021

Keywords:
Atrial fibrillation
Fibroblast
Equine
Structural remodeling

ABSTRACT

Background: Fibroblasts maintain the extracellular matrix homeostasis and may couple to cardiomyocytes through gap junctions and thereby increase the susceptibility to slow conduction and cardiac arrhythmias, such as atrial fibrillation (AF). In this study, we used an equine model of persistent AF to characterize structural changes and the role of fibroblasts in the development of an arrhythmogenic substrate for AF.

Material and methods: Eleven horses were subjected to atrial tachypacing until self-sustained AF developed and were kept in AF for six weeks. Horses in sinus rhythm (SR) served as control. In terminal open-chest experiments conduction velocity (CV) was measured. Tissue was harvested and stained from selected sites. Automated image analysis was performed to assess fibrosis, fibroblasts, capillaries and various cardiomyocyte characteristics.

Results: Horses in SR showed a rate-dependent slowing of CV, while in horses with persistent AF this rate-dependency was completely abolished (CV•basic cycle length relation $p = 0.0295$). Overall and interstitial amounts of fibrosis were unchanged, but an increased fibroblast count was found in left atrial appendage, Bachmann's bundle, intraatrial septum and pulmonary veins ($p < 0.05$ for all) in horses with persistent AF. The percentage of α-SMA expressing fibroblasts remained the same between the groups.

Conclusion: Persistent AF resulted in fibroblast accumulation in several regions, particularly in the left atrial appendage. The increased number of fibroblasts could be a mediator of altered electrophysiology during AF. Targeting the fibroblast proliferation and differentiation could potentially serve as a novel therapeutic target slowing down the structural remodeling associated with AF.

1. Introduction

Atrial fibrillation (AF) is a common cardiac arrhythmia in humans which has a progressive nature [1]. Initially AF is induced by triggered activity and is self-terminating, but may progress over time to more persistent forms [2]. Electrical and structural remodeling processes are identified as important factors for AF progression. Fibroblasts are commonly acknowledged for their role in the production of fibrous tissue and structural remodeling [3]. However, fibroblasts have lately also gained attention in the field because they might contribute to the cardiac electrical properties [4,5].

Fibroblasts have an important role in tissue homeostasis as they control the composition and structure of the extracellular matrix (ECM) [6]. Generally, two types of atrial fibrosis are recognized: interstitial fibrosis and replacement fibrosis [7]. Interstitial fibrosis, most commonly reported in AF patients and animal models [8–11], results in increased transverse separation of cardiomyocyte bundles (perimysial fibrosis), but can also lead to increased separation of cardiomyocytes within bundles (endomysial fibrosis). Increased cellular distance between cardiomyocytes due to endomysial

* Corresponding author.
E-mail address: rib@sund.ku.dk (R. Buhl).

https://doi.org/10.1016/j.ijcha.2021.100842
2352-9067/

fibrosis results in altered electrical impulse propagation, mainly in the transverse direction [10,12].

Beside the important role in the ECM homeostasis, fibroblasts are also believed to be coupled to cardiomyocytes and are therefore assumed to have an active contribution to cardiac electrophysiological properties [13]. The electrical coupling between cardiomyocytes and fibroblasts is believed to be mediated through gap junctions composed of connexin isoforms 40, 43 and 45 [14]. Fibroblasts are not excitable, but a variety of ion channels contribute to a resting membrane potential of approximately −30 mV [15]. Dependent on the phase of the action potential of the cardiomyocyte, coupled fibroblasts will either lead to a slight depolarization (phase 4) or an accelerated early repolarization (phase 1 and 2). At tissue levels increased fibroblast density may therefore cause slowed conduction [16,17], promote re-entries [17] and favor ectopic activity [4].

Over the last couple of years, the horse has gained increasing interest as a large animal model of arrhythmias [18–22]. In contrast to other animal models usually used in AF research, such as rodents, pigs, dogs and goats, horses are frequently reported to develop AF spontaneously, just like humans [23–26]. Furthermore, spontaneous pulmonary vein firings were recorded in a horse recently, indicating that AF triggering processes might resemble the ones in humans, which supports the horse as a highly suitable and interesting animal for AF research [27].

In this study, we used a horse model of persistent AF to gain increased understanding of atrial structural remodeling, fibroblasts and their role in the electrical and structural remodeling during persistent AF. We aimed to perform a comprehensive cellular analysis in five different regions of the equine heart. Additionally, we investigated if atrial contractile function was impaired and whether it had any correlation to the structural remodeling happening during persistent AF.

2. Material and methods

2.1. Animals

The experiments were performed under animal license authorized by the Danish Animal Inspectorate (license number 2016-15-0201-01128) and in accordance with the EU legislations for animal protection and care and was approved by a local ethics committee.

Three groups were included in this study; 1) horses in persistent AF used for CV recordings and tissue comparison 2) healthy horses used for control tissue samples 3) healthy horses in SR used for reference CV recordings in the atrium. Group 1 consisted of eleven horses with induced AF that had already been enrolled in a forerunning AF study [28], group 2 consisted of nine healthy horses in SR and group 3 consisted of six healthy horses from a Danish abattoir (Fig. 1). All three groups were sex-and age-matched.

For horses in group 1, persistent AF was induced as previously described [28]. In short, eleven retired Standardbred racehorses (mean age: 7 ± 2.5 yr) had an implantable pacing device inserted and were subsequently subjected to atrial tachypacing (600 bpm) until AF was self-sustained (time to self-sustained AF: 6 ± 4 days). Self-sustained AF was defined as AF that was self-maintained for more than 24hr without rapid atrial tachypacing. At day 29 cardioversion was attempted with an $I_{K,ACh}$ blocker (XAF-1407) as part of another study and in case of successful cardioversion echocardiography was performed. Shortly after the horses were paced back into AF and kept in this state for 42.3 ± 4.7 days until euthanasia.

2.2. Conduction velocity

The horses in group 1 and 3 underwent an open-chest surgical procedure [29], where the right atrium (RA) was mapped epicardially for the assessment of CV using a 49-electrode high density mapping array (inter-electrode distance of 2.5 mm). Conduction maps were recorded during pacing (2x threshold) at 400, 500 and 1000 ms basic cycle length (BCL). The pacing site had 2.5 mm distance to the map to assure an epicardial wavefront during measurements. In total nine horses from the AF group were successfully mapped as well as nine horses from the SR group. Horses in the AF group were electrically cardioverted just prior to CV measurements. The horses were euthanized by exsanguination after the CV recordings.

2.3. Echocardiography

The horses included in the AF group underwent echocardiographic (ECHO) examinations at baseline in SR before implantation of the pacer and in SR just after cardioversion on day 29 [28]. All examinations were performed by one experienced operator using a portable Vivid I ultrasound system (GE Healthcare, Denmark) and were performed in standing, non-sedated horses with a resting heart rate of 45 bpm or lower. Subsequently, blinded data analysis was carried out offline using EchoPac (GE Healthcare, Denmark). Two-dimensional ECHO variables for the assessment of LA size and function were measured as follows: left atrial area at mitral valve closure (LAA_{min}), left atrial area at onset of the P wave (LAA_a), left atrial area at mitral valve opening (LAA_{max}), passive left atrial fractional area change ($LA\text{-}FAC_{passive} = (LAA_{max}–LAA_a)/LAA_{max}$), active left atrial fractional area change ($LA\text{-}FAC_{active} = (LAA_a–LAA_{min})/LAA_a$) and total left atrial fractional area change ($LA\text{-}FAC_{total} = (LAA_{max}– LAA_{min})/LAA_{max}$).

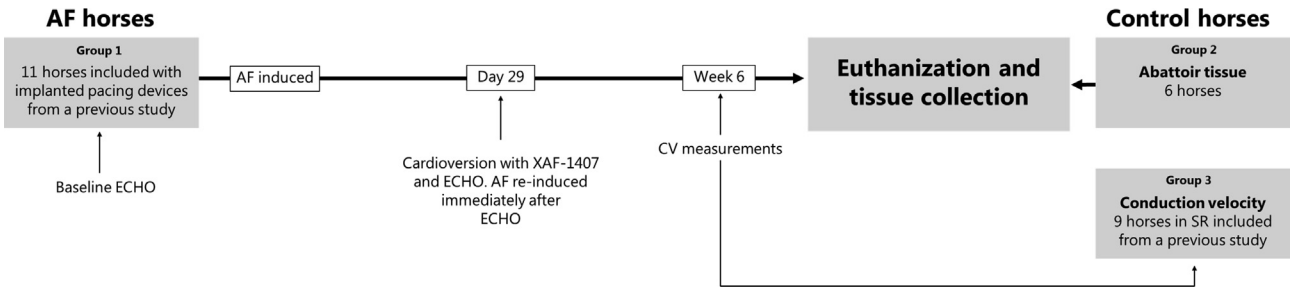

Fig. 1. Overview of animals included and procedures performed. AF horses were included from a previous study [28]. Two different groups of horses were used as control. One group was used for the tissue comparison and consisted of horses from a Danish abattoir. The other group was used for CV measurement and was included from a previous study. AF: atrial fibrillation; CV: conduction velocity; ECHO: echocardiography; SR: sinus rhythm.

2.4. Histology and immunohistochemistry

Within 15 min of euthanasia, tissue was harvested and snap-frozen in liquid nitrogen or formalin-fixed from the following locations: left atrial appendage (LAapp), right atrial appendage (RAapp), Bachmann's bundle (BB), interatrial septum (IAS) and pulmonary veins (PV). For histological staining, formalin-fixed and paraffin-embedded tissue was sectioned at 4 μm and stained with Sirius red in order to assess the total amount of fibrosis. In order to identify fibroblasts, amount of ECM and capillaries we used a newly developed method by Winters et al. [30]. Frozen tissue was sectioned at 8 μm, fixed in ice-cold acetone for 10 min and washed with Phosphate Buffered Saline (PBS). Blocking was performed by incubation with 2% (w/v) fraction V bovine serum albumin and 2% (w/v) glycine in PBS at room temperature for 1 h. To identify fibroblasts the sections were incubated with primary anti-vimentin antibody (1:150) (Rabbit Monoclonal to vimentin, Abcam) overnight. The following day, the sections were incubated at room temperature with secondary fluorescein-labelled anti-vimentin secondary antibody (1:200) (Goat Anti-Rabbit IgG Cross Absorbed, Alexa Flour 405, Thermo Fisher). To identify the cell membrane of cardiomyocytes and ECM the sections were incubated with WGA diluted in PBS (1:200) (Alexa Flour 594 conjugate, ThermoFisher) for 2 h at room temperature. To stain capillaries, sections were incubated with GS-IB4 diluted in PBS (1:200) (Isolectin GS-IB4, Alexa Flour 488 conjugate, ThermoFisher) for 2 h. Coverslips were mounted with Prolong Gold (ProLong™ Gold antifade reagent, Invitrogen).

Next we sought to investigate and quantify the number of α-smooth muscle actin (α-SMA) expressing fibroblasts. In order to do so, α-SMA and vimentin positive cells were identified. Staining was performed using formalin-fixed and paraffin-embedded tissue, cut at 4 μm. After deparafinization, antigen retrieval was performed by boiling the sections in an acetate buffer (pH = 6.0). Blocking was performed by incubation with 2% (w/v) fraction V bovine serum albumin and 2% (w/v) glycine in PBS at room temperature for 1 h. Following the blocking procedure, the sections were incubated with primary anti-vimentin antibody (1:150) (Rabbit Monoclonal to vimentin, Abcam) and α-SMA (1:500) (Mouse monoclonal to α-smooth muscle actin, Abcam) overnight at 4° C diluted in blocking buffer. The following day, the sections were incubated with secondary antibodies (1:1000) (Goat Anti-Rabbit IgG Cross Absorbed, Alexa Flour 568 and Goat Anti-Mouse IgG Highly Cross Absorbed, Alexa Flour 647) for 2 h at room temperature. Coverslips were mounted with Prolong Gold (ProLong™ Gold antifade reagent, Invitrogen).

2.5. Epifluorescence microscopy and automated image analysis

Sections stained with Sirius Red were imaged using the Zeiss Axio Scan.Z1 Slide scanner at 10x magnification. Images were analyzed using the ZEN Intellessis software as described previously [22]. Overall amounts of fibrosis were quantified based on the whole tissue section, which included both epicardial as well as perivascular fibrosis. Interstitial amounts of fibrosis were analyzed in 5 areas of each section avoiding the epicardial and perivascular fibrosis. For the analysis of the triple staining (WGA, vimenin and GS-IB4), epifluorescence microscopy was performed using an upright Leica DM4B combined with a Leica MC170HD camera and LAS v4.8 imaging software. Automated analysis of the generated images was performed using a custom-coded algorithm for ImageJ, which was recently tested and validated in a goat model of AF [30]. For each section 2–6 randomly selected fields were analyzed. Only fields with cardiomyocytes cut in the transverse direction were included in the analysis. WGA staining served as base for overall ECM quantification, cardiomyocyte count and size as well as inter-myocyte distance used as an indirect measure for interstitial fibrosis (Fig. 2**A**). The vimentin staining was used to visualize fibroblasts and to quantify the number of fibroblasts per surface area (Fig. 2**B**), while the GS-IB4 staining was used to label capillaries and to quantify capillary count and size (Fig. 2**C**).

For the subsequent detection and analysis of α-SMA expressing fibroblasts, the stained sections were imaged using the Zeiss Axio Scan.Z1 Slide scanner with fluorescence microscopy and a 20x/0.8 objective. For each tissue section 5 randomly selected fields were analyzed. Only fields with cardiomyocytes cut in the transverse direction were included in the analysis. Likewise, fields containing vessels were also not included in the analysis. Also for this analysis ZEN Intellessis software was applied in order to keep the analysis automated.

2.6. Statistical analysis

For statistical analysis GraphPad Prism ed.8 (GraphPad Software, USA) was used. Results are given as mean ± standard error of mean (SEM). Statistical analyses are indicated in the figure legends. In all statistical analysis p-values < *0.05* were considered to be statistically significant.

3. Results

3.1. Conduction velocity

To investigate the electrophysiological changes following persistent AF we measured RA CV during the terminal open-chest experiments. The relationship between CV and BCL was found to be flattened in AF horses indicating that healthy horses have a rate dependent slowing of CV, while this rate dependency is abolished in horses with persistent AF (CV•basic cycle length relation $p = 0.0295$) (Fig. 3**A**). Furthermore, the CV was slower at 1000 ms BCL ($p = 0.0109$) in horses with persistent AF.

3.2. Contractile changes after six weeks of persistent AF in horses

Echocardiography was performed in order to evaluate cardiac dimensions and function. The active and overall emptying function of the left atrium (LA) was found to be significantly reduced in horses cardioverted to SR after 29 days of AF. LA-FAC_{active} was decreased ($p < 0.0001$, Fig. 3**B**), whereas no significant change in LA-$FAC_{passive}$ was observed (Fig. 3**C**). Overall atrial function (LA-FAC_{total}) decreased significantly after 29 days of AF ($p < 0.05$) (Fig. 3**D**).

The left atrial area at mitral valve closing (LAA_{min}) and the left atrial area at mitral valve opening (LAA_{max}) were both unchanged upon 29 days of AF, which indicates unchanged LA dimensions in the horses with persistent AF (data not shown).

3.3. Structural changes after six weeks of persistent AF in horses

As we in a previous study observed that 8 weeks of tachypacing-induced AF resulted in significant increases in fibrosis both in RAapp and in LAapp we initially investigated whether the same was the case in our model after 6 weeks of AF. However, in none of the five investigated regions we could find a significant change in the amount of overall fibrosis (Fig. 4). When looking at interstitial fibrosis we likewise did not find any significant changes in the amount of fibrosis, although clear tendencies can be observed in both LAapp, BB, IAS and PV, but not in RAapp, with an average of 9.0% increase in interstitial fibrosis in all of these regions (Fig. 5).

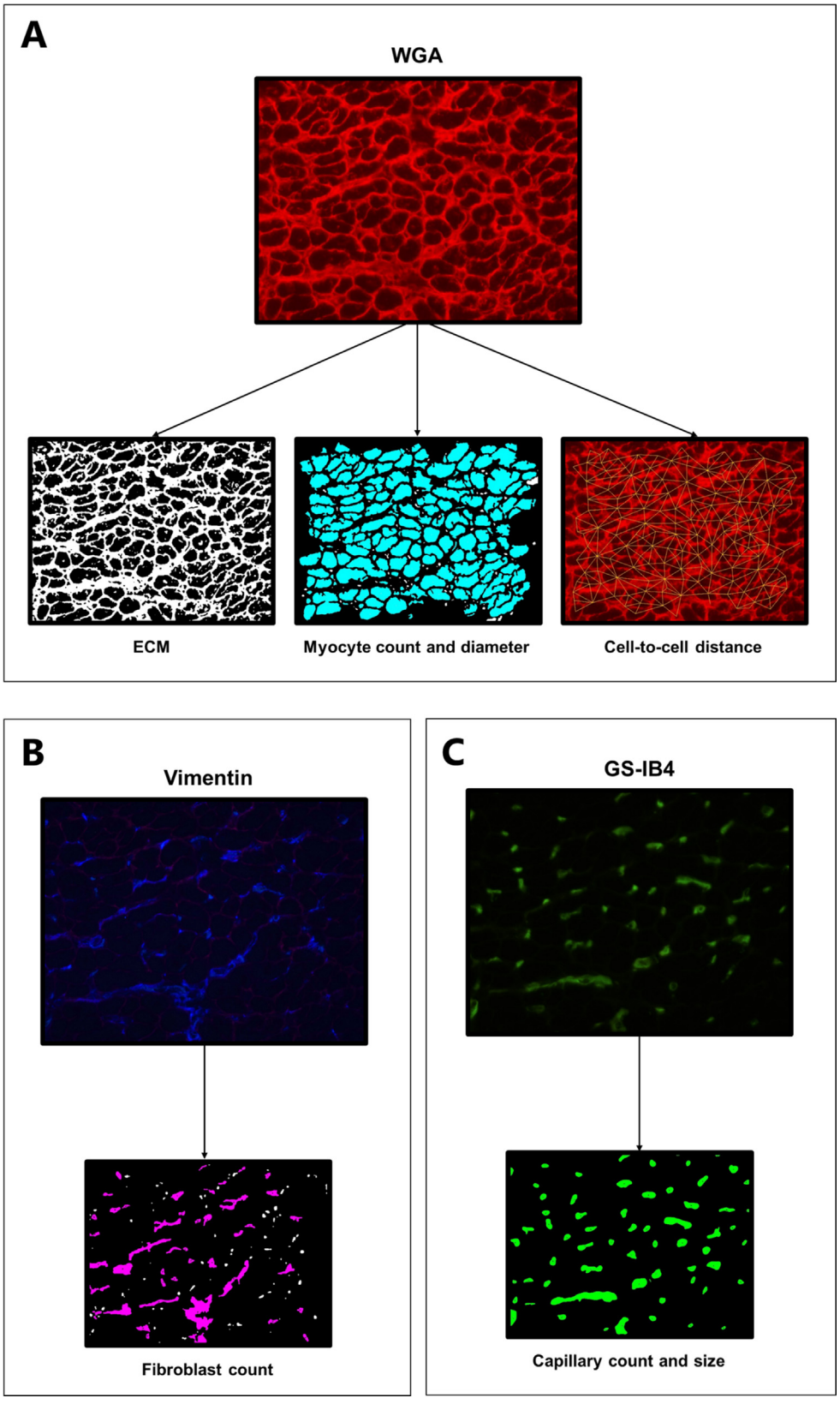

Fig. 2. Representative images of the immunohistochemical triple labeling of (A) extracellular matrix (WGA), (B) fibroblasts (vimentin) and (C) capillaries (GS-IB4) and the subsequent automated offline analysis in ImageJ (lower panels). In the first image in the lower panel in A the phansalker threshold has been applied allowing separation of ECM (white) and cardiomyocytes (black). Subsequently the size of each cardiomyocyte can be determined as well as the distance to neighboring cardiomyocytes. In the lower panel of B and C the original images for fibroblast and capillaries have been segmented using the Landini algorithm for HSB thresholding. The vimentin positive images are corrected for unspecific endothelial staining as they are subtracted from the GS-IB4 images. ECM: extracellular matrix; WGA: wheat germ agglutinin.

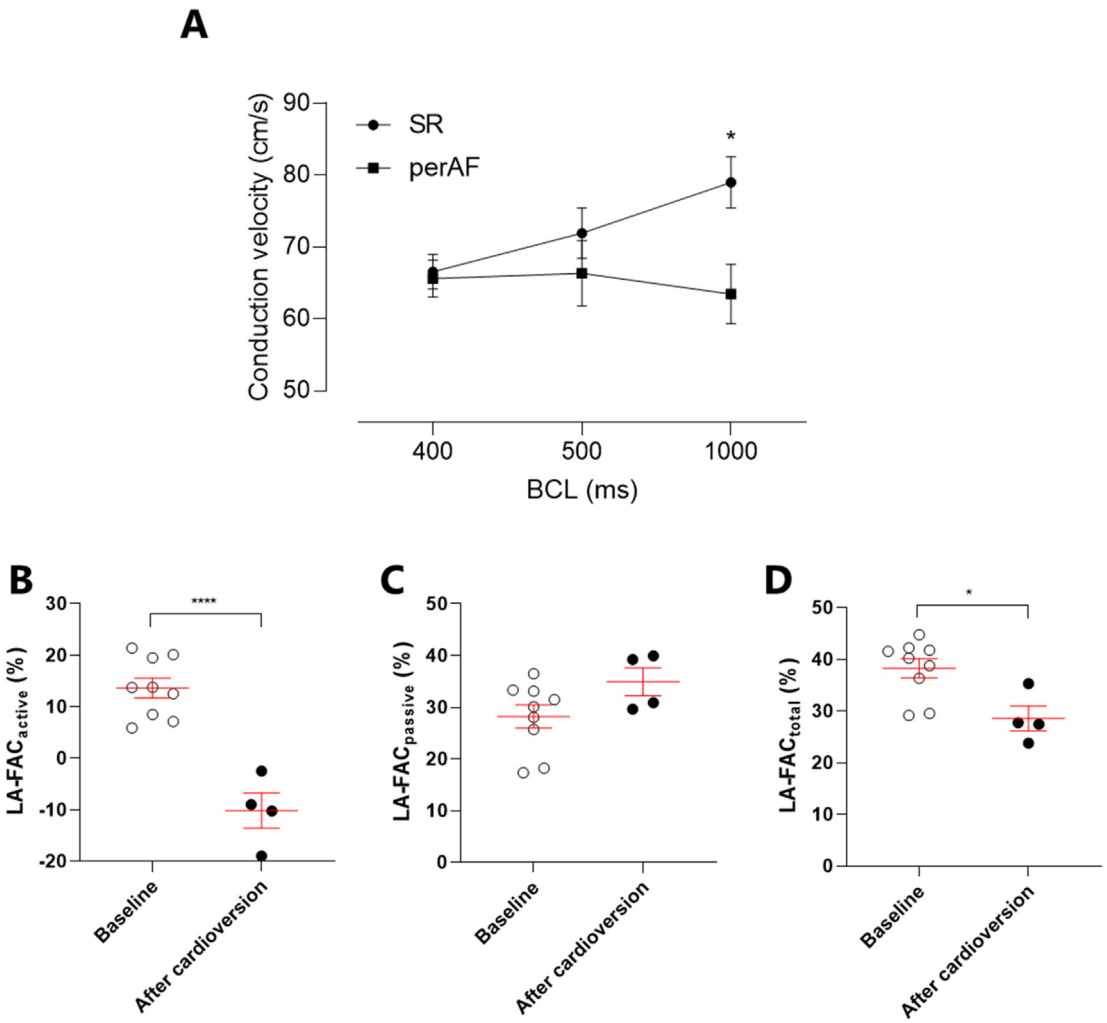

Fig. 3. Changes in atrial conduction velocity following persistent AF (A) and echocardiographic evaluation (B). (A) Healthy horses have a rate dependent slowing of CV, while in horses with persistent AF this rate dependency is completely abolished. Statistical analysis was performed using a mixed-effects analysis to compare conduction velocity between SR and AF at 400, 500 and 1000 ms BCL. (B) Changes in LA function (top) and LA dimensions (bottom). Echocardiography was performed during SR. Statistical analysis was performed using unpaired *t*-test. LA-FAC_{active}: left atrial fractional change describing active atrial contraction; LA-$FAC_{passive}$: left atrial fractional change describing passive atrial emptying; LA-FAC_{total}: left atrial fractional change describing overall atrial function; LA_{min}: describing left atrial diameter at mitral valve closure; LA_{max}: describing left atrial diameter at mitral valve opening; AF: atrial fibrillation; BCL: basic cycle length; LA: left atrium; perAF: persistent AF; SR: sinus rhythm. $^{*} = p < 0.05$ *and* $^{****} = p < 0.0001$.

3.4. Increased fibroblast accumulation in several regions of the heart after six weeks of persistent AF in horses

Immunohistochemistry was performed on sections from five different regions of the heart. The distribution of fibroblasts were in general found to be fairly uniform, but the highest level was found in the RAapp (Fig. 6). Compared with control hearts, an increased number of fibroblasts per surface area was found in LAapp, BB, IAS and PV ($p < 0.05$ for all) in the hearts from the AF horses. Although not significant, the same tendency was observed in RAapp ($p = 0.075$) (Fig. 6).

When normalized to myocyte count the lowest relative levels were found in the LAapp, PV and IAS, while the levels in BB and RA were two-fold higher. Compared to the hearts of control horses, the horses with persistent AF had a significantly increased number of fibroblasts per cardiomyocyte (fibroblast density) in LAapp ($p < 0.05$) and same tendency was observed in PV ($p = 0.079$) (Fig. 6).

Next, we investigated if these fibroblasts and vimentin positive cells also were expressing α-SMA, which is commonly recognized as a marker of activated fibroblasts, namely the myofibroblast. We found that the portion of α-SMA expressing fibroblasts to be similar between the groups at all sites investigated with a mean of 23.8 ± 4.8% in the control group vs. 23.1 ± 2.9% in the AF group. This indicates that the cardiac fibroblasts not yet have differentiated into the active myofibroblasts which is in accordance with the fact that we do not observe increased levels of fibrosis in the tissue. A representative image of α-SMA expressing fibroblasts can be found in (Fig. 7).

3.5. Extracellular matrix changes after six weeks of persistent AF in horses

Six weeks of persistent AF did don induce changes in the amount of ECM in the regions analyzed (Figs. 8 and 9). The WGA staining served as base for overall ECM quantification and was also used to determine the inter-myocyte distance and used as an indirect measure of interstitial fibrosis. These results are in line with what we observe with the Sirius red staining. Only the cardiomyocyte diameter in LAapp was found to be decreased in the AF horses ($p < 0.05$), which could indicate cellular atrophy in this region (Figs. 8 and 9). To investigate whether AF was associated

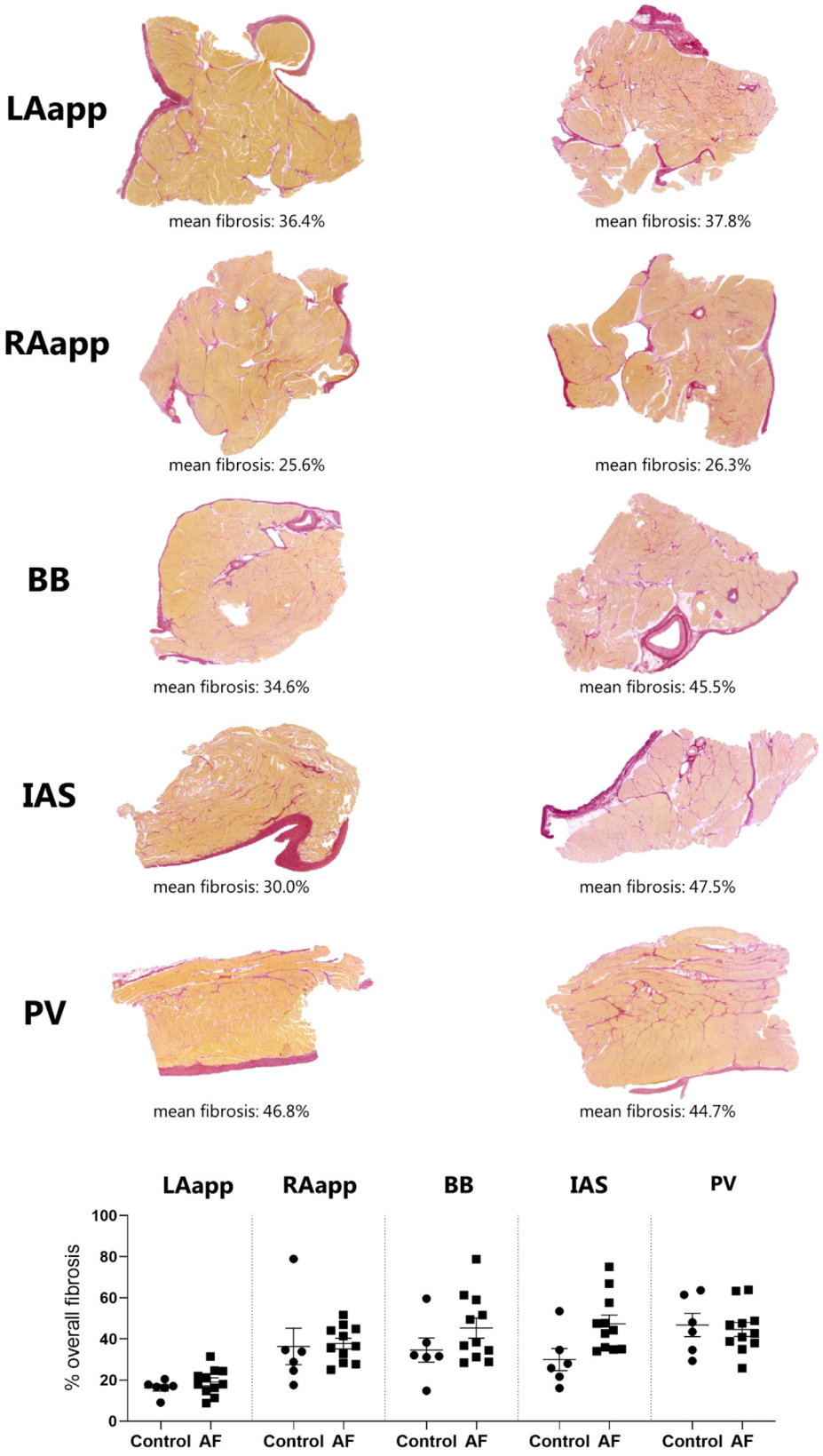

Fig. 4. No changes in overall fibrosis after 6 weeks of induced AF. Collagen was visualized using Sirius red and total amount of fibrosis was quantified using deep learning by Zen Intellesis. Statistical analysis was performed by repeated t-testing and corrected using the Holm-Sidak method without assuming a consistent SD. LAapp: left atrial appendage; RAapp: right atrial appendage; BB: Bachmann's Bundle; IAS: intra atrial septum; PV: pulmonary vein.

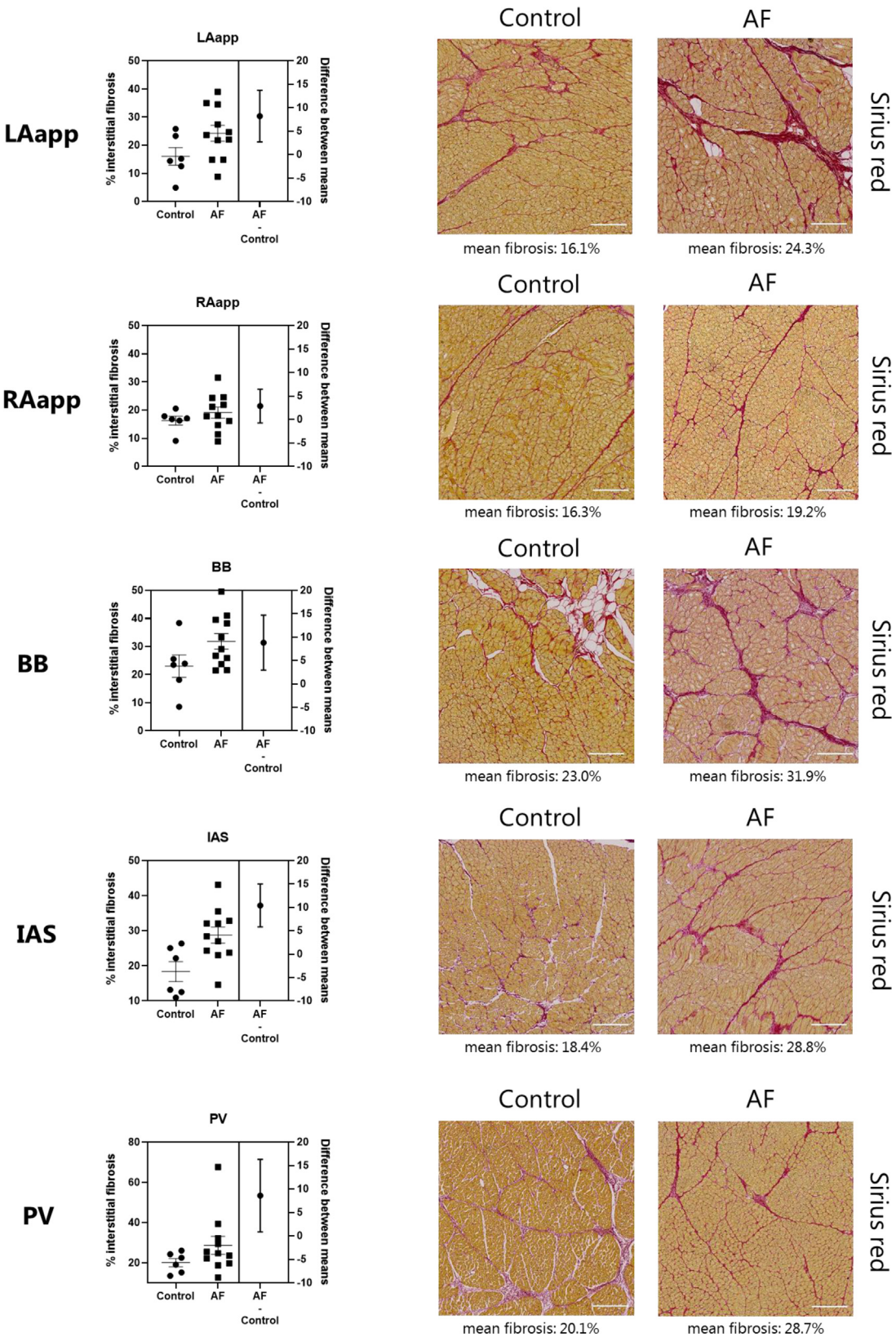

Fig. 5. Amount of intersitial fibrosis remains unchanged after 6 weeks of induced AF. Collagen was visualized using Sirius red and the amount of interstitial fibrosis was quantified using deep learning by Zen Intellesis. For each section 5 randomly selected areas were analyzed. Statistical analysis was performed by repeated t-testing and corrected using the Holm-Sidak method without assuming a consistent SD. LAapp: left atrial appendage; RAapp: right atrial appendage; BB: Bachmann's Bundle; IAS: intra atrial septum; PV: pulmonary vein. Scale bar 200 μm.

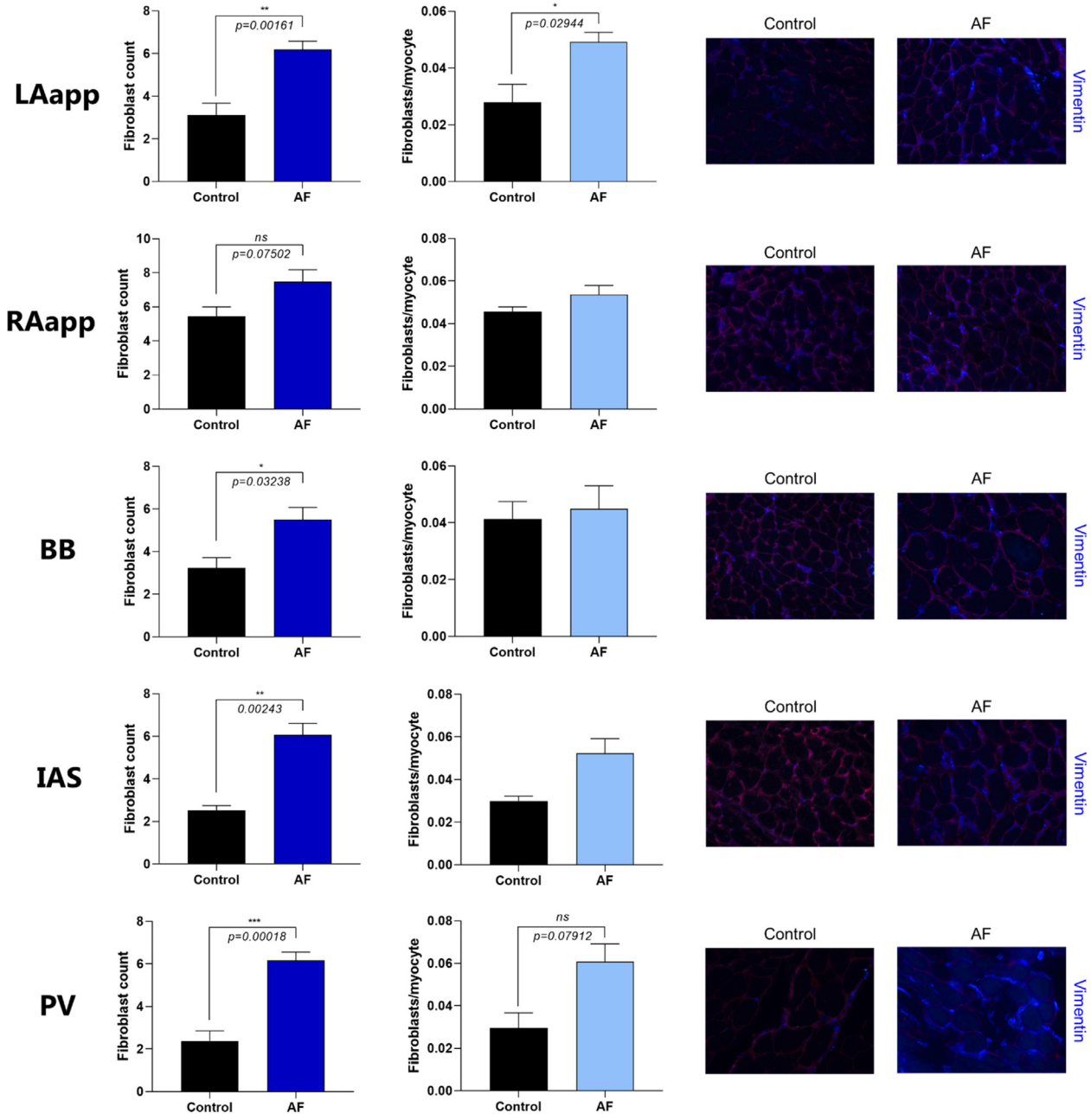

Fig. 6. Increased fibroblast accumulation in several regions of the equine heat. Persistent AF results in increased accumulation of fibroblasts in LAapp, BB, IAS and PV and in an increased number of fibroblasts per cardiomyocyte in LAapp (fibroblast density). Left panel shows representative vimentin images from control and AF hearts from each site investigated. Statistical analysis was performed by repeated t-testing and corrected using the Holm-Sidak method without assuming a consistent SD. LAapp: left atrial appendage; RAapp: right atrial appendage; BB: Bachmann's Bundle; IAS: intra atrial septum; PV: pulmonary vein. * =$p < 0.05$, ** = $p < 0.01$, *** = $p < 0.001$.

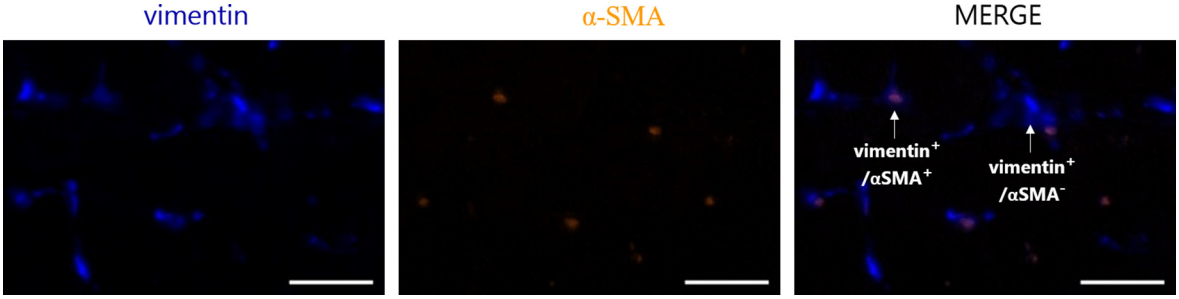

Fig. 7. Representative image of α-SMA expressing fibroblasts in the equine heart. Scale bar 20 μm.

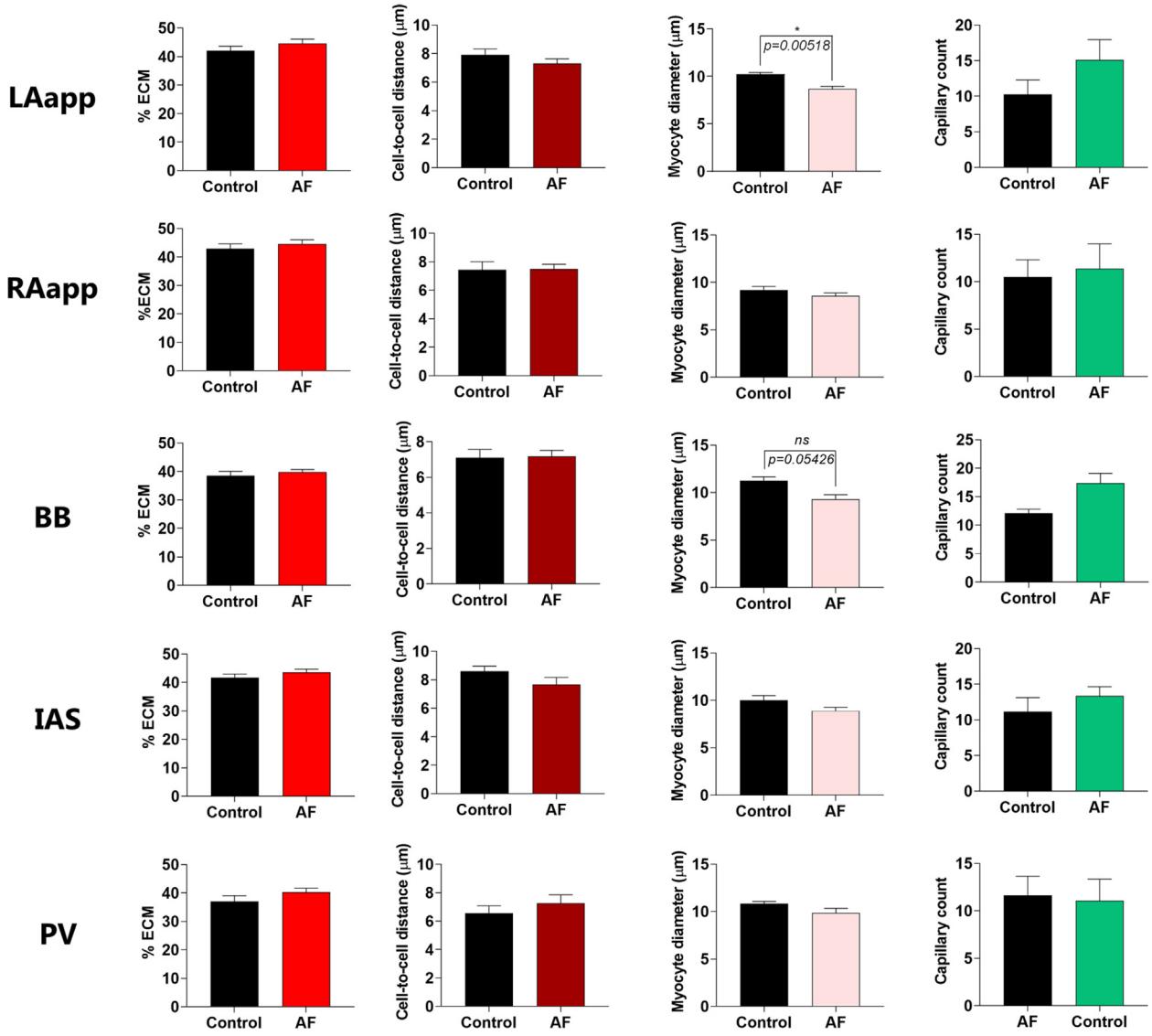

Fig. 8. Myocardial changes following persistent AF. In this model persistent AF did not increase overall fibrosis, endomysioal fibrosis (cell–cell distance) nor cell size. Number of capillaries did not differ in any of the investigated regions. Statistical analysis was performed by repeated t-testing and corrected using the Holm-Sidak method without assuming a consistent SD. LAapp: left atrial appendage; RAapp: right atrial appendage; BB: Bachmann's Bundle; IAS: intra atrial septum; PV: pulmonary vein. * *=p < 0.05.*

with an altered distribution of vascularization we also quantified the number of capillaries per surface area. Capillaries were similarly distributed in all regions and did not differ significantly between the horses with persistent AF and control horses (Figs. 8 and 9).

4. Discussion

In this study, we investigated whether regional differences in structural remodeling could serve as mediator of altered atrial electrophysiology following six weeks of persistent AF. We found that both the atrial CV as well as atrial contractility was reduced, but we did not find any signs of structural remodeling. On the other hand we did find increased fibroblast accumulation in several regions of the myocardium following six weeks of persistent AF.

As recent *in silico* studies have suggested, increased fibroblast density might affect the electrical properties of the myocardium [17,31]. Especially the LA seems to be affected by an increase in fibroblast density, as block of action potential propagation occurred more frequently in the LA than in other regions [17]. We investigated changes in atrial CV *in vivo* and were able to demonstrate a distinct difference between horses in SR and horses that had been in AF for six weeks. Healthy horses in SR showed a rate dependent slowing of CV, while for horses with persistent AF this rate dependency was completely abolished. This study also confirmed an overall decrease in cardiac contractile function, but no changes in LA dimensions. Changes in contractile function in the early phase of AF can largely be attributed to reduction of L-type Ca^{2+} channel current and loss of sarcomeres (myolysis) [11,32,33]. In tachypaced dogs, a 70% reduction in I_{CaL} was found after six weeks of AF [34]. As I_{CaL} plays an important role in the release of Ca^{2+} from the sarcoplasmic reticulum, a reduced I_{CaL} is expected to result in a reduced activation of the contractile apparatus. Likewise myolysis is believed to lead to a reduction in the contractile force [32].

The slowing of CV in horses with persistent AF may be explained by increased accumulation of cardiac fibroblasts in several regions including LAapp, PV, BB and IAS, confirmed by

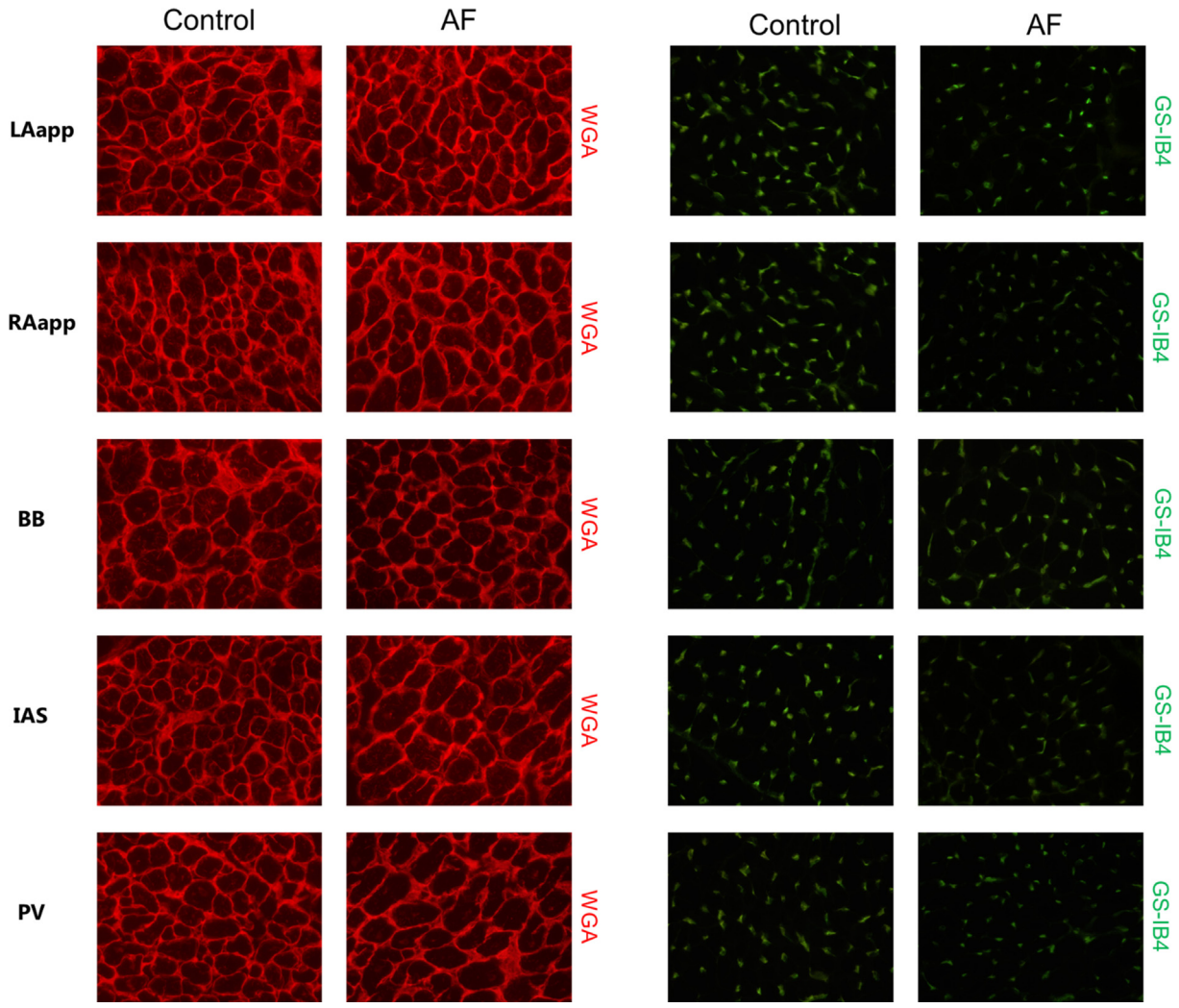

Fig. 9. Representative WGA and GS-IB4 images from sites examined. LAapp: left atrial appendage; RAapp: right atrial appendage; BB: Bachmann's bundle; IAS: intra atrial septum; PV: pulmonary vein; WGA: wheat germ agglutinin.

immunofluorescence. The same tendency was observed in RAapp, however not significantly. In LAapp, the increased accumulation of fibroblasts also resulted in increased number of fibroblasts per cardiomyocyte (fibroblast density). However, as no changes in the amount of overall nor interstitial fibrosis were observed, the changes in CV might be attributed to the increased fibroblast accumulation or the stretch caused by the loss of contractility. We cannot explicitly claim that the increased number of fibroblasts is the only explanation for the changes observed in CV as many other factors, such as electrical remodeling and changes in connexin expression, also can influence CV and stabilize AF [35]. Previously, increased amounts of both interstitial and overall atrial fibrosis have been observed in horses upon 2 months of AF [22]. In goats, increased amounts of endomysial fibrosis in the epicardium was found after six months of AF, while three weeks of AF did not induce any fibrotic changes [10]. The first signs of AF related remodeling are typically reported to be cellular hypertrophy and changes in connexin expression and distribution, while the formation of fibrotic tissue follows after some weeks or months of AF [32]. This study puts forward the notion that increased fibroblast accumulation could be an early sign of AF induced structural remodeling and that fibroblasts also potentially are actively contributing to alteration in atrial electrophysiology. Why fibroblast proliferation is induced by the onset of AF needs further investigation. A range of different stimuli is able to induce fibroblast proliferation, including as angiotensin (II) (Ang(II)), endothelin-1 and basic growth factor (TGF-β1), [36,37] that in turn can activate a range of different transcriptional factors, such as the Smad transcription factors [38]. The importance of Ca^{2+} has in several studies been highlighted for both fibroblast proliferation and differentiation [39,40]. The Ca^{2+} signaling in fibroblasts is most likely mediated by the transient receptor potential (TRP) channels [36]. Especially the TRPM7 subfamily seems to be important and as it is several fold upregulated during AF [41]. Suppression of the TRPM7 current results in inhibition of both the TGF-β1-induced proliferation and differentiation of fibroblast [41]. This indicates that suppression of TRPM7 channels might be a promising target for inhibiting fibroblast proliferation and thereby also production of collagen in AF.

Besides being involved in cardiac electrophysiology and the homoeostasis of the ECM, fibroblasts also contribute to the regulation of cardiac vessels. The formation of capillaries, known as angiogenesis, can be regulated by fibroblast secreting factors. One of these factors the vascular endothelial growth factor (VEGF), which induces angiogenesis, has been found to be increased in AF patients [42–45]. In this study, we also found a tendency to increased numbers of capillaries in LAapp and BB. A few studies have previously investigated the alterations in vasculature during

AF. Pigs subjected to atrial tachypacing and kept in AF for approximately six weeks had an increase in capillary density in RA and the same tendency was observed in LA [46]. Data from human studies are however pointing towards another direction either showing no change or even a reduction in capillary number [47–51]. It has been proposed that capillary density varies depending on the stage of AF [52]. Initially, during early stages of AF the atrial oxygen demand increases and an increase in angiogenic signaling leads to a formation of new capillaries to meet the increased demand [52]. Despite increased levels of VEGF during paroxysmal AF, these levels decrease in patients with persistent AF [53]. Additionally, new capillaries do not remain unless they are stabilized by pericyte interaction [52]. So, the initial commensurate increase in capillary amount to meet the increase in oxygen demand does not persist leading to the well-known state of atrial oxygen supply–demand ischemia in AF.

Even though the present study demonstrated an increased fibroblast accumulation after six weeks of AF in the PV, the functional impact remains unclear. Whether cardiomyocytes in the PV are coupled to fibroblasts in the native cardiac tissue or if they only contribute to the increased production of fibrosis found in the PV tissue of AF patients remains unanswered [54]. In computational studies the PVs have also been found to be highly affected by increased fibroblast density [17].

In this study we showed that six weeks of persistent AF resulted in both reduced contractile function as well as reduced atrial CV. Furthermore, we found increased fibroblast accumulation without any other structural changes. Hesselkilde et al. [22] found increased amounts of fibrosis after 8 weeks of persistent AF. Based on this we speculate whether in the early stages of AF (few weeks) the fibroblasts are mainly affecting the cardiac electrophysiology through direct electrical coupling, while in the later stages (weeks to months) they also contribute to the structural remodeling by increasing fibrosis deposition.

5. Limitations

In this study we were only able to conduct CV recordings of RA, which is an impediment of this study as the electrophysiological properties of RA and LA vary and observations made in one atrium cannot always be directly translated to the other. Furthermore, it is a limitation that different control groups were included and that CV data was measured in one group, while tissue analysis was performed in another control group. Determining the fibroblast/myocyte ratio based on immunohistochemical sections do not take the 3 dimensional structure of the cell into account. Although fibroblasts are highly abundant they are also very small and therefore the sink effect could be irrelevant, but this calls for further investigation.

6. Conclusion

To our knowledge, this is the first study showing regional differences in structural remodeling following persistent AF. In horses, six weeks of persistent AF is associated with increased accumulation of fibroblasts, but not any changes in the amount of fibrosis, in several regions of the heart including LAapp, PV, BB and IAS. Understanding the impact of fibroblasts on atrial electrophysiology as well as their role in atrial structural remodeling in the early phases of AF, might prove to be a key element in AF management.

Funding

The study was funded by the European Union's Horizon 2020 MSCA ITN under Grant Agreement No. 675351, The Independent Research Fund Denmark, DFF-7017–00050, The Kustos Foundation of 1881, Kirsten og Freddy Johansens Fond and Svenningsens Fond.

Declaration of Competing Interest

The authors declare that they have no known competing financial interests or personal relationships that could have appeared to influence the work reported in this paper.

Acknowledgement

We acknowledge the assistance and facilities provided by the Core Facility for Integrated Microscopy (CFIM) at the Faculty of Health and Medical Sciences, University of Copenhagen, Denmark.

References

[1] A.D. Margulescu, L. Mont, Persistent atrial fibrillation vs paroxysmal atrial fibrillation: differences in management, Expert review of cardiovascular therapy. 15 (8) (2017) 601–618.
[2] P. Kirchhof, S. Benussi, D. Kotecha, A. Ahlsson, D. Atar, B. Casadei, et al., 2016 ESC Guidelines for the Management of Atrial Fibrillation Developed in Collaboration With EACTS, Revista espanola de cardiologia (English ed). 70 (1) (2017) 50.
[3] U. Schotten, S. Verheule, P. Kirchhof, A. Goette, Pathophysiological mechanisms of atrial fibrillation: a translational appraisal, Physiol. Rev. 91 (1) (2011) 265–325.
[4] C. Poulet, S. Künzel, E. Büttner, D. Lindner, D. Westermann, U. Ravens, Altered physiological functions and ion currents in atrial fibroblasts from patients with chronic atrial fibrillation, Physiological reports. 4 (2) (2016).
[5] M.B. Thomsen, K. Calloe, Human atrial fibroblasts and their contribution to supraventricular arrhythmia, Physiological reports. 4 (3) (2016).
[6] P. Camelliti, T.K. Borg, P. Kohl, Structural and functional characterisation of cardiac fibroblasts, Cardiovasc. Res. 65 (1) (2005) 40–51.
[7] S. Nattel, Molecular and Cellular Mechanisms of Atrial Fibrosis in Atrial Fibrillation, JACC Clinical electrophysiology. 3 (5) (2017) 425–435.
[8] M.S. Spach, J.P. Boineau, Microfibrosis produces electrical load variations due to loss of side-to-side cell connections: a major mechanism of structural heart disease arrhythmias, Pacing and clinical electrophysiology : PACE. 20 (2 Pt 2) (1997) 397–413.
[9] J. Ausma, H.M. van der Velden, M.H. Lenders, E.P. van Ankeren, H.J. Jongsma, F. C. Ramaekers, et al., Reverse structural and gap-junctional remodeling after prolonged atrial fibrillation in the goat, Circulation 107 (15) (2003) 2051–2058.
[10] S. Verheule, J. Eckstein, D. Linz, B. Maesen, E. Bidar, A. Gharaviri, et al., Role of endo-epicardial dissociation of electrical activity and transmural conduction in the development of persistent atrial fibrillation, Prog. Biophys. Mol. Biol. 115 (2–3) (2014) 173–185.
[11] U. Schotten, J. Ausma, C. Stellbrink, I. Sabatschus, M. Vogel, D. Frechen, et al., Cellular mechanisms of depressed atrial contractility in patients with chronic atrial fibrillation, Circulation 103 (5) (2001) 691–698.
[12] D.H. Lau, D. Linz, U. Schotten, R. Mahajan, P. Sanders, J.M. Kalman, Pathophysiology of Paroxysmal and Persistent Atrial Fibrillation: Rotors, Foci and Fibrosis, Heart, lung & circulation. 26 (9) (2017) 887–893.
[13] C.A. Souders, S.L. Bowers, T.A. Baudino, Cardiac fibroblast: the renaissance cell, Circ. Res. 105 (12) (2009) 1164–1176.
[14] R.D. Johnson, P. Camelliti, Role of Non-Myocyte Gap Junctions and Connexin Hemichannels in Cardiovascular Health and Disease: Novel Therapeutic Targets? International journal of molecular sciences. 19 (3) (2018).
[15] S. Chacar, N. Farès, P. Bois, J.F. Faivre, Basic Signaling in Cardiac Fibroblasts, J. Cell. Physiol. 232 (4) (2017) 725–730.
[16] J. Pellman, J. Zhang, F. Sheikh, Myocyte-fibroblast communication in cardiac fibrosis and arrhythmias: Mechanisms and model systems, J. Mol. Cell. Cardiol. 94 (2016) 22–31.
[17] J. Sanchez, J.F. Gomez, L. Martinez-Mateu, L. Romero, J. Saiz, B. Trenor, Heterogeneous Effects of Fibroblast-Myocyte Coupling in Different Regions of the Human Atria Under Conditions of Atrial Fibrillation, Front. Physiol. 10 (2019) 847.
[18] M.M. Haugaard, S. Pehrson, H. Carstensen, M. Flethøj, E.Z. Hesselkilde, K.F. Praestegaard, et al., Antiarrhythmic and electrophysiologic effects of flecainide on acutely induced atrial fibrillation in healthy horses, J. Vet. Intern. Med. 29 (1) (2015) 339–347.
[19] M.M. Haugaard, E.Z. Hesselkilde, S. Pehrson, H. Carstensen, M. Flethøj, K.F. Præstegaard, et al., Pharmacologic inhibition of small-conductance calcium-activated potassium (SK) channels by NS8593 reveals atrial antiarrhythmic potential in horses, Heart rhythm. 12 (4) (2015) 825–835.
[20] E.Z. Hesselkilde, H. Carstensen, M.M. Haugaard, J. Carlson, S. Pehrson, T. Jespersen, et al., Effect of flecainide on atrial fibrillatory rate in a large animal model with induced atrial fibrillation, BMC cardiovascular disorders. 17 (1) (2017) 289.

[21] I. Vernemmen, D. De Clercq, A. Decloedt, L. Vera, G. Van Steenkiste, G. van Loon, Atrial premature depolarisations five days post electrical cardioversion are related to atrial fibrillation recurrence risk in horses, Equine Vet. J. 52 (3) (2020) 374–378.
[22] E.Z. Hesselkilde, H. Carstensen, M. Flethøj, M. Fenner, D.D. Kruse, S.M. Sattler, et al., Longitudinal study of electrical, functional and structural remodelling in an equine model of atrial fibrillation, BMC cardiovascular disorders. 19 (1) (2019) 228.
[23] R. Buhl, S.D. Nissen, M.L.K. Winther, S.K. Poulsen, C. Hopster-Iversen, T. Jespersen, et al., Implantable loop recorders can detect paroxysmal atrial fibrillation in Standardbred racehorses with intermittent poor performance, Equine Vet. J. (2020).
[24] A.A. Leroux, J. Detilleux, C.F. Sandersen, L. Borde, R.M. Houben, A. Al Haidar, et al., Prevalence and risk factors for cardiac diseases in a hospital-based population of 3,434 horses (1994–2011), J. Vet. Intern. Med. 27 (6) (2013) 1563–1570.
[25] P. Physick-Sheard, M. Kraus, P. Basrur, K. McGurrin, D. Kenney, F. Schenkel, Breed predisposition and heritability of atrial fibrillation in the Standardbred horse: a retrospective case-control study, Journal of veterinary cardiology : the official journal of the European Society of Veterinary Cardiology. 16 (3) (2014) 173–184.
[26] A. Saljic, T. Jespersen, R. Buhl, Anti-arrhythmic investigations in large animal models of atrial fibrillation, Br. J. Pharmacol. (2021).
[27] D. Linz, E. Hesselkilde, R. Kutieleh, T. Jespersen, R. Buhl, P. Sanders, Pulmonary vein firing initiating atrial fibrillation in the horse: Oversized dimensions but similar mechanisms, J. Cardiovasc. Electrophysiol. 31 (5) (2020) 1211–1212.
[28] M.F. Fenner, H. Carstensen, S.D. Nissen, E.Z. Hesselkilde, C. Lunddahl, M.A. Jensen, et al., Effect of Selective I(K, ACh) Inhibition by XAF-1407 in an Equine Model of Tachypacing-induced Persistent Atrial Fibrillation (AF), Br. J. Pharmacol. (2020).
[29] D.M.T. Adler, K. Hopster, C. Hopster-Iversen, M. Fenner, R. Buhl, S. Jacobsen, Thoracotomy and Pericardiotomy for Access to the Heart in Horses: Surgical Procedure and Effects on Anesthetic Variables, Journal of equine veterinary science. 96 (2021) 103315.
[30] J. Winters, M.E. von Braunmuhl, S. Zeemering, M. Gilbers, T.T. Brink, B. Scaf, et al., JavaCyte, a novel open-source tool for automated quantification of key hallmarks of cardiac structural remodeling, Sci. Rep. 10 (1) (2020) 20074.
[31] Y. Xie, A. Garfinkel, P. Camelliti, P. Kohl, J.N. Weiss, Z. Qu, Effects of fibroblast-myocyte coupling on cardiac conduction and vulnerability to reentry: A computational study, Heart rhythm. 6 (11) (2009) 1641–1649.
[32] M. Allessie, J. Ausma, U. Schotten, Electrical, contractile and structural remodeling during atrial fibrillation, Cardiovasc. Res. 54 (2) (2002) 230–246.
[33] J. Ausma, M. Wijffels, F. Thoné, L. Wouters, M. Allessie, M. Borgers, Structural changes of atrial myocardium due to sustained atrial fibrillation in the goat, Circulation 96 (9) (1997) 3157–3163.
[34] L. Yue, J. Feng, R. Gaspo, G.R. Li, Z. Wang, S. Nattel, Ionic remodeling underlying action potential changes in a canine model of atrial fibrillation, Circ. Res. 81 (4) (1997) 512–525.
[35] T. Kato, Y.K. Iwasaki, S. Nattel, Connexins and atrial fibrillation: filling in the gaps, Circulation 125 (2) (2012) 203–206.
[36] L. Yue, J. Xie, S. Nattel, Molecular determinants of cardiac fibroblast electrical function and therapeutic implications for atrial fibrillation, Cardiovasc. Res. 89 (4) (2011) 744–753.
[37] B. Burstein, E. Libby, A. Calderone, S. Nattel, Differential behaviors of atrial versus ventricular fibroblasts: a potential role for platelet-derived growth factor in atrial-ventricular remodeling differences, Circulation 117 (13) (2008) 1630–1641.
[38] J. Massagué, How cells read TGF-beta signals, Nat. Rev. Mol. Cell Biol. 1 (3) (2000) 169–178.
[39] Olson ER, Shamhart PE, Naugle JE, Meszaros JG. Angiotensin II-induced extracellular signal-regulated kinase 1/2 activation is mediated by protein kinase Cdelta and intracellular calcium in adult rat cardiac fibroblasts. Hypertension (Dallas, Tex : 1979). 2008;51(3):704-11.
[40] F.J. Ramires, Y. Sun, K.T. Weber, Myocardial fibrosis associated with aldosterone or angiotensin II administration: attenuation by calcium channel blockade, J. Mol. Cell. Cardiol. 30 (3) (1998) 475–483.
[41] J. Du, J. Xie, Z. Zhang, H. Tsujikawa, D. Fusco, D. Silverman, et al., TRPM7-mediated Ca2+ signals confer fibrogenesis in human atrial fibrillation, Circ. Res. 106 (5) (2010) 992–1003.
[42] G. Krenning, E.M. Zeisberg, R. Kalluri, The origin of fibroblasts and mechanism of cardiac fibrosis, J. Cell. Physiol. 225 (3) (2010) 631–637.
[43] B. Freestone, A.Y. Chong, H.S. Lim, A. Blann, G.Y. Lip, Angiogenic factors in atrial fibrillation: a possible role in thrombogenesis?, Ann Med. 37 (5) (2005) 365–372.
[44] N.A. Chung, F. Belgore, F.L. Li-Saw-Hee, D.S. Conway, A.D. Blann, G.Y. Lip, Is the hypercoagulable state in atrial fibrillation mediated by vascular endothelial growth factor?, Stroke 33 (9) (2002) 2187–2191
[45] Y. Seko, H. Nishimura, N. Takahashi, T. Ashida, R. Nagai, Serum levels of vascular endothelial growth factor and transforming growth factor-beta1 in patients with atrial fibrillation undergoing defibrillation therapy, Jpn. Heart J. 41 (1) (2000) 27–32.
[46] C. Citerni, J. Kirchhoff, L.H. Olsen, S.M. Sattler, F. Gentilini, M. Forni, et al., Characterization of Atrial and Ventricular Structural Remodeling in a Porcine Model of Atrial Fibrillation Induced by Atrial Tachypacing, Frontiers in veterinary science. 7 (2020) 179.
[47] F. Gramley, J. Lorenzen, B. Jedamzik, K. Gatter, E. Koellensperger, T. Munzel, et al., Atrial fibrillation is associated with cardiac hypoxia, Cardiovascular pathology : the official journal of the Society for Cardiovascular Pathology. 19 (2) (2010) 102–111.
[48] A. Olasinska-Wisniewska, T. Mularek-Kubzdela, S. Grajek, A. Marszalek, W. Sarnowski, M. Jemielity, et al., Impact of atrial remodeling on heart rhythm after radiofrequency ablation and mitral valve operations, The Annals of thoracic surgery. 93 (5) (2012) 1449–1455.
[49] D. Corradi, S. Callegari, R. Maestri, S. Benussi, S. Bosio, G. De Palma, et al., Heme oxygenase-1 expression in the left atrial myocardium of patients with chronic atrial fibrillation related to mitral valve disease: its regional relationship with structural remodeling, Hum. Pathol. 39 (8) (2008) 1162–1171.
[50] D. Corradi, S. Callegari, R. Maestri, D. Ferrara, D. Mangieri, R. Alinovi, et al., Differential structural remodeling of the left-atrial posterior wall in patients affected by mitral regurgitation with or without persistent atrial fibrillation: a morphological and molecular study, J. Cardiovasc. Electrophysiol. 23 (3) (2012) 271–279.
[51] A. Boldt, A. Scholl, J. Garbade, M.E. Resetar, F.W. Mohr, J.F. Gummert, et al., ACE-inhibitor treatment attenuates atrial structural remodeling in patients with lone chronic atrial fibrillation, Basic Res. Cardiol. 101 (3) (2006) 261–267.
[52] D. Opacic, K.A. van Bragt, H.M. Nasrallah, U. Schotten, S. Verheule, Atrial metabolism and tissue perfusion as determinants of electrical and structural remodelling in atrial fibrillation, Cardiovasc. Res. 109 (4) (2016) 527–541.
[53] A. Scridon, E. Morel, E. Nonin-Babary, N. Girerd, C. Fernandez, P. Chevalier, Increased intracardiac vascular endothelial growth factor levels in patients with paroxysmal, but not persistent atrial fibrillation, Europace : European pacing, arrhythmias, and cardiac electrophysiology : journal of the working groups on cardiac pacing, arrhythmias, and cardiac cellular electrophysiology of the European Society of Cardiology. 14 (7) (2012) 948–953.
[54] R.J. Hassink, H.T. Aretz, J. Ruskin, D. Keane, Morphology of atrial myocardium in human pulmonary veins: a postmortem analysis in patients with and without atrial fibrillation, J. Am. Coll. Cardiol. 42 (6) (2003) 1108–1114.